Experimental Coupling and Decoupling of Engineering Structures using Frequency-Based Substructuring

[1]S. Manzato,[1,2]C. Napoli, [2]G. Coppotelli, [2]A. Fregolent, [3]W. D'Ambrogio, [1]B. Peeters

[1]Siemens Industry Software NV, Interleuvenlaan 68, 3001, Leuven, Belgium
[2]Università degli Studi di Roma "La Sapienza", Dipartimento di Ingegneria Meccanica e Aerospaziale, Via Eudossiana 18, 00184 Roma, Italy
[3]Università degli Studi dell'Aquila, DIIE, Via G. Gronchi 18, I 67100 L'Aquila, Italy

ABSTRACT
In many engineering application there are many instances in which it is convenient to be able to consider a complex engineering structure as an assembly of simpler components or substructures. Similarly, there exist applications in which, for model validation purposes, it might be important to identify the dynamic behavior of the structural subsystem starting from the known dynamic behavior of the coupled system and from information about the remaining part of the structural system. However, if the theoretical framework for Frequency Based Substructuring (FBS) has been widely studied and demonstrated, measurement errors, ill-conditioning and difficulties in measuring all required degrees of freedom – in particular at the connections – lead to poor results when trying to apply these techniques to real structures. This paper will focus on the analysis of the results obtained by applying Experimental Frequency-Based Substructuring on a test structure, both for coupling and decoupling applications and under different boundary conditions. The paper will particularly discuss the effects of typical measurement errors on the final results and potential techniques that could be used to improve the robustness and applicability of this methodology.

KEYWORDS: Substructuring, FBS, Coupling, Decoupling, Experimental Validation

1. INTRODUCTION

Dynamic Substructuring (DS) is a topic deeply developed from the theoretical point of view in the last forty years. It is based on the componentwise analysis of a structural system, and in particular:

- too large or complex systems can be partitioned, in order to avoid a high computational time or a big effort from the numerical/experimental point of view;
- DS allows the identification of local dynamic behaviors and the representation of a simplified dynamics;
- parts modeled in a different way (discretized or analytical) can be combined, performing an hybrid analysis; components can be developed by different project teams, with the possibility to combine them as final step.

Dynamic Substructuring can be divided in two branches: coupling and decoupling. Coupling is applied when one wants to know the characteristics of a structure formed by simpler components (called substructures or subsystems), while decoupling has to deal with the inverse problem: to know more about a substructure, starting from the investigation of the assembled structure and of the "residual" part.
Whilst analytical substructuring forms the basis of the Finite Element Method and related techniques (i.e. the Craig-Bampton method), Experimental/Analytical Substructuring is less widely applied, as it requires that at least one of the substructures is experimentally identified. As the method generally requires the inversion of a matrix, ill-conditioning, measurement errors and difficulties in measuring all required degrees of freedom have limited the application of the method to real industrial cases. These applications range from the possibility of combining

experimental and numerical models of substructures to predict the coupled dynamic response [1] to the possibility of subtracting the dynamic behavior of a fixture when a component is connected to it to facilitate its testing [2]. Moreover, wind turbine manufactures can be interested of predicting the effect of installing a new gearbox on a wind turbine. As gearboxes are usually tested by manufacturers on dedicated test-rig, if they can be first decoupled from the rig and then coupled on the turbine (either numerically or experimentally modeled), possible coupling problems could be identified before the turbines are installed [3].
This list is not at all comprehensive of all possible practical applications of analytical/experimental dynamic substructuring, but gives only an idea of the range of possible applications and problems that could be solved. Recently, de Klerk et al. [4] have summarized 50 years of dynamic substructuring and classified the different methods, providing a general framework and outlining the relations between them. In [3-6], current bottlenecks in the application of dynamic substructuring to experimental data are discussed and possible solutions that could improve the quality of the results proposed.
This paper will focus on Frequency-Based Substructuring (FBS) methods, aiming at a validation of substructuring procedures from the experimental point of view, carrying out a test activity and suggesting the field of applicability of the aforementioned procedures. In section 2, some of these methods are summarized, both for coupling and decoupling of substructures. Some numerical techniques to improve the quality of the matrix inversion will also be presented. In section 3, these techniques will be applied on real FRFs acquired on an experimental structure. The results will be reviewed and analyzed with the use of some mathematical tools. Some practical guidelines and lessons learned will be then summarized to design future experimental campaigns.

2. THEORETICAL BACKGROUND

The theoretical foundations of Frequency Based Substructuring are widely presented in literature and the methods implemented and used in this paper can be found in [7] for the substructure coupling problem and in [3], [4] and [8] for the decoupling. Only the most important equations will be here reported for clarity.

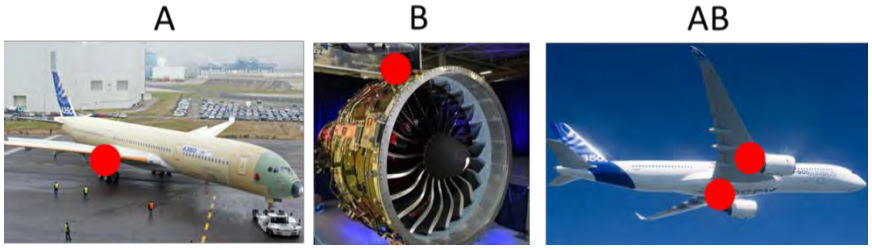

Fig. 1: Example of subsystem A and B combined into the coupled structure AB. The red dots indicate the connection points.

2.1 FREQUENCY-BASED SUBSTRUCTURING USING THE DUAL FORMULATION

As shown in Figure 1, let's consider 3 different models: models A and B, which represent two substructures or components, and model AB, which is the assembled structures obtained by connecting A and B at some degrees of freedom. The equation of motion of a general substructure is expressed in the physical domain as:

$$M^{(s)}\ddot{u} + C^{(s)}\dot{u} + K^{(s)}u = f^{(s)} + g^{(s)} \tag{1}$$

Where M, C and K are respectively the mass, damping and stiffness matrix, u are the degrees of freedom and f and g the external and internal forces applied at each degree of freedom. Similarly, the assembled behavior of n substructures that are to be coupled can be rewritten in a block-diagonal format as:

$$M\ddot{u} + C\dot{u} + Ku = f + g \tag{2}$$

Moreover, the degrees of freedom (dof) u of the two substructures A and B to be assembled can be conveniently order as:

- ua: internal dofs to substructure A;
- uc: dofs connecting the two substructures;
- ub: internal dofs to substructure B.

The compatibility condition can be expressed as:

$$Bu = 0 \tag{3}$$

where the B matrix operates on the interface dofs and is a signed Boolean matrix if the interface dofs are matching. Similarly, the equilibrium condition is expressed as:

$$L^T g = 0 \tag{4}$$

where the matrix L is the Boolean matrix localizing the interface dofs of the substructures in the global dual set of dofs. By using a dual assembly formulation, the full set of global dofs is retained, so that all interface dofs uc are present as many times as there are subdomains connected on the corresponding node. The dual assembled system is thus obtained by satisfied a priori the interface equilibrium by choosing the interface forces in the form:

$$g = -B^T \lambda \tag{5}$$

where λ are Lagrange multipliers corresponding physically to the interface forces intensities. Including the condition in Eq. (5), the system of equations built using Eq. (2), (3) and (4) and expressing the coupled behavior of two or more substructures can be expressed in the dual formulation as:

$$\begin{cases} M\ddot{u} + C\dot{u} + Ku + B^T \lambda = f \\ Bu = 0 \end{cases} \tag{6}$$

The dual formulation for the behavior of coupled substructures expressed in Eq.(6) in the physical domain can be written in the frequency domain as:

$$\begin{bmatrix} Z & B^T \\ B & 0 \end{bmatrix} \begin{bmatrix} u \\ \lambda \end{bmatrix} = \begin{bmatrix} f \\ 0 \end{bmatrix} \tag{7}$$

where Z is now the block-diagonal matrix containing the dynamic stiffness matrices of the substructures. In experimental structural dynamics, one usually computes Frequency Response Functions H by applying a force and measuring accelerations at specific points of the structures and dynamic stiffness information (which is the inverse of the receptance FRFs) is not readily available. Thus, eliminating the Lagrange multipliers in the system of equation (7), one finds the so-called dual interface problem in the frequency domain, suitable for the coupling of accelerance matrices H(ω) obtained with experimental data:

$$u = Hf - HB^T \left(BHB^T \right)^{-1} BHf = \overline{H} f \tag{8}$$

By taking advantage of the distinction between internal and connecting dofs, Eq.(8) can be rewritten in a more extended and clear form to directly compute the accelerance matrix of the coupled structure AB from the measured accelerance matrices of the two substructures A and B as:

$$\overline{H} = H^{AB} = \begin{bmatrix} H_{aa}^{AB} & H_{ac}^{AB} & H_{ab}^{AB} \\ H_{ca}^{AB} & H_{cc}^{AB} & H_{cb}^{AB} \\ H_{ba}^{AB} & H_{bc}^{AB} & H_{bb}^{AB} \end{bmatrix} = \begin{bmatrix} H_{aa}^{A} & H_{ac}^{A} & 0 \\ H_{ca}^{A} & H_{cc}^{A} & 0 \\ 0 & 0 & H_{bb}^{B} \end{bmatrix} - \begin{bmatrix} H_{ac}^{A} \\ H_{cc}^{A} \\ -H_{bc}^{B} \end{bmatrix} \left[H_{cc}^{A} + H_{cc}^{B} \right]^{-1} \begin{bmatrix} H_{ac}^{A} \\ H_{cc}^{A} \\ -H_{bc}^{B} \end{bmatrix}^T \tag{9}$$

With reference to Figure 1, Eq. (9) allows to calculate the dynamic response of the coupled system AB from the known dynamic response of structure A and B. Substructure decoupling (that is deriving the response of subsystem B from the known AB and A systems) is derived as a particular case of Eq. (9), where now substructure A is subtracted from the coupled system AB. The standard interface decoupling method, where equilibrium and compatibility conditions are solely applied to the connecting dofs, can be written as:

$$H_{CC}^{B}=\begin{bmatrix} H_{aa}^{B} & H_{ac}^{B} & H_{ab}^{B} \\ H_{ca}^{B} & H_{cc}^{B} & H_{cb}^{B} \\ H_{ba}^{B} & H_{bc}^{B} & H_{bb}^{B} \end{bmatrix}=\begin{bmatrix} H_{aa}^{AB} & H_{ac}^{AB} & H_{ab}^{AB} \\ H_{ca}^{AB} & H_{cc}^{AB} & H_{cb}^{AB} \\ H_{ba}^{AB} & H_{bc}^{AB} & H_{bb}^{AB} \end{bmatrix}-\begin{bmatrix} H_{ac}^{AB} \\ H_{cc}^{AB} \\ H_{bc}^{AB} \end{bmatrix}\left[H_{cc}^{AB}-H_{cc}^{A}\right]^{-1}\begin{bmatrix} H_{ac}^{AB} \\ H_{cc}^{AB} \\ H_{bc}^{AB} \end{bmatrix}^{T} \tag{10}$$

Note in particular that by explicitly writing down Eq. (10), the first column and row of the resulting dynamic matrix of substructure B correspond to the internal dofs of subsystem A when additional interface forces are applied and can be neglected for simplicity as they are usually not of interest.

2.2. NUMERICAL IMPROVEMENTS OF THE GENERAL METHODS

The solution of Eq. (9) and (10) requires that all connection dofs FRFs are accessible and measurable and that the matrix inversion problem required to solve the method is well conditioned. Whilst these problems can be neglected when dealing with analytical or numerical FRFs, they can create serious error or even completely hamper the dynamic substructuring results when one deals with experimentally measured FRFs. An overview of these problems and possible solutions proposed by different research groups can be found in [3-6] and [9]. One of the most important problems in experimental substructuring is that the rotational dofs at the connection point are seldom measurable in an accurate fashion, thus not all the required information can be measured. Typically, two solutions were identified in literature to solve this problem: estimating these rotational FRFs by modal expansion techniques [5] or by applying the so-called Equivalent Multi-Point connection method [10]. These solutions are not applied here and will be the objective of future investigations. A further solution, only valid for decoupling problems, is to substitute unmeasured rotational dofs at connection points with internal dofs of the residual substructure A [15], as in the subsequent Eqs. (11) and (12). The second problem is purely numerical and is related to the inversion of the matrix. This is related to the ill-conditioning of the problem and the generally high condition number of the FRF matrix, in particular in correspondence of resonance, causes the inverse solution to be very sensitive even to small perturbations. As measured FRFs will always contain some amount of noise, the Moore-Penrose pseudoinverse based on the singular value decomposition is commonly used instead of the standard inverse.

Over the years, several methods have been proposed to improve the quality of experimental substructuring by imposing the equilibrium and compatibility conditions (Eqs. (3) and (4)) not only to the connection dofs but also to additional internal dofs of the residual substructure A. Using the standard interface approach for decoupling, the connection forces between the substructures are determined only using the minimum information needed, that is the responses on the interface dofs. In [3], [8] and [9] it is shown that by using this relaxed interface approach is possible to exploit information coming from other points of the structure, thus solving an overdetermined problem when inverting the matrix. This will then require the use of the Moore-Penrose pseudoinverse (as the matrix is not square anymore) with a tolerance on the lower singular value to be included in the inversion. The smaller singular values in fact usually correspond to large term in the inverse and can lead to numerical errors in the solution. Of course the selection of the lower singular value to be included is based on a compromise choice between condition number and accuracy of the estimation and depends on the specific application. Some more details on the methods, as well as on an alternative regularization, are given in [11].

A first example of these relaxed interfaces is the so-called Extended Interface, where additional internal dofs of the residual structure A are considered in the compatibility and equilibrium conditions:

$$H_{AC,AC}^{B}=\begin{bmatrix} H_{aa}^{AB} & H_{ac}^{AB} & H_{ab}^{AB} \\ H_{ca}^{AB} & H_{cc}^{AB} & H_{cb}^{AB} \\ H_{ba}^{AB} & H_{bc}^{AB} & H_{bb}^{AB} \end{bmatrix}-\begin{bmatrix} H_{aa}^{AB} & H_{ac}^{AB} \\ H_{ca}^{AB} & H_{cc}^{AB} \\ H_{ba}^{AB} & H_{bc}^{AB} \end{bmatrix}\left[\begin{bmatrix} H_{aa}^{AB} & H_{ac}^{AB} \\ H_{ca}^{AB} & H_{cc}^{AB} \end{bmatrix}-\begin{bmatrix} H_{aa}^{A} & H_{ac}^{A} \\ H_{ca}^{A} & H_{cc}^{A} \end{bmatrix}\right]^{+}\begin{bmatrix} H_{aa}^{AB} & H_{ac}^{AB} \\ H_{ca}^{AB} & H_{cc}^{AB} \\ H_{ba}^{AB} & H_{bc}^{AB} \end{bmatrix}^{T} \tag{11}$$

where the symbol +denotes the pseudo-inverse. Both the Standard and Extended interface method are collocated, as compatibility and equilibrium conditions are enforced on the same points. This condition is however not strictly required and compatibility and equilibrium can be enforced on different dofs in a so-called non-collocated approach. A method can also be derived by enforcing the equilibrium and compatibility only on internal dofs of subsystem A:

$$H_{A,A}^{B} = \begin{bmatrix} H_{aa}^{AB} & H_{ac}^{AB} & H_{ab}^{AB} \\ H_{ca}^{AB} & H_{cc}^{AB} & H_{cb}^{AB} \\ H_{ba}^{AB} & H_{bc}^{AB} & H_{bb}^{AB} \end{bmatrix} - \begin{bmatrix} H_{aa}^{AB} \\ H_{cc}^{AB} \\ H_{ba}^{AB} \end{bmatrix} \left[H_{aa}^{AB} - H_{aa}^{A} \right]^{+} \begin{bmatrix} H_{aa}^{AB} \\ H_{cc}^{AB} \\ H_{ba}^{AB} \end{bmatrix}^{T} \tag{12}$$

The advantage of this method is that it neglects the connection FRFs in the inversion problem, thus improving the robustness of the inversion. These FRFs, as can be observed, will still need to be measured to allow the decoupling.

3. EXPERIMENTAL DATA ANALYSIS

In literature[12], the sensitivity of frequency based substructuring to small errors (e.g. noise, spykes,etc.) on the measured FRFs is widely reported. In a previous publication from the authors [13] this trend was also confirmed both by analyzing numerical and experimental results and the requirement for extremely high quality measurements was stressed. In this paper, these findings were applied on the structure shown in **Fig. 2** with the objective of demonstrating that, with enough care in the acquisition of FRFs, FBS can be applied and accepatable results can be obtained. Some numerical and experimental previous works on the same structure are discussed in [14] and [15]; with this paper, the objective is to expand the results using different methods and boundaries conditions.
The analyzed aluminum structure is composed of:

- A beam, considered as substructure B (the long horizontal beam on top of **Fig. 2**;
- A beam with two short horizontal arms near the connection point (11), considered as substructure A;
- Screws and washers at the connection area to simulate a rigid interface.

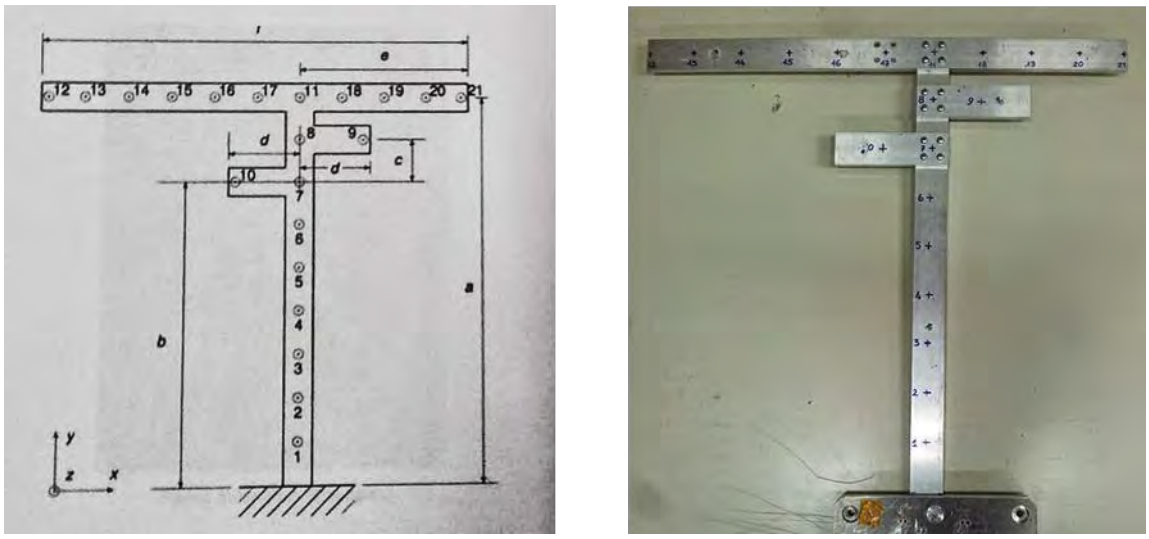

Fig. 2: The selected test structure (left) with its dimensions (right)

The geometrical dimensions are reported in Table 1. The applied technique is impact testing: to this end, roving hammer is used, and both clamped and free-free boundary conditions will be assumed for the assembled structure AB and for substructure A, while substructure B will be always tested in free-free conditions to have reference values after decoupling. FRFs are measured in the frequency range 0-2048 Hz with a spectral resolution of 0.5 Hz. The beam B is suspended to a metal frame in the horizontal position, using some soft rubber bands to approximate free-free boundaries. Four mono-directional accelerometers are placed at the connection point #11 (Z direction) and at points #13, #16 and #20 (Z direction), as in Fig 2. As regards the assembled structure AB, points #3, #6, #9, #10, #11, #13, #16 and #20 are chosen, hence points #3, #6, #9, #10 and #11 are considered for substructure A. It can also be noticed that:

- it is possible to hit on the upper part of the item and to measure exactly on the same location on the lower part, also at the connection;
- the material has no discontinuities or superficial defects;
- the surface to hit is flat.

Table 1: Geometrical dimension of the tested structure.

Dimensions	[mm]
a	540
b	420
c	60
d	100
e	240
l	600

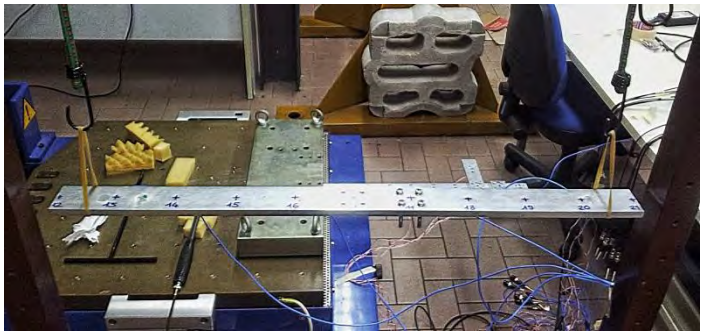

Fig. 3: Substructure B suspended on soft bungees.

3.1. MEASURED FRFs ANALYSIS

During the acquisition of the FRFs, particular attention was put in:

- quality of the driving point FRF at each impact location (impact direction and location, similar input spectrum).
- Reciprocity.

Both these properties are at the basis of each experimental analysis with FRFs, but, as clearly discussed in literature [12], they become extremely critical in Frequency-Based Substructuring applications and have a very high sensitivity on the results. **Fig. 4** compare the reciprocal FRFs for the assembled structure between a point on substructure A and a point on substructure B for both boundary conditions. The displayed FRFs cover the 0-1300 Hz band, as at higher frequencies the reciprocity is relatively poor. In this range, the FRFs nicely overlap at resonances, but they differ at the anti-resonances and in particular in the band from 400 to 600 Hz. Also, the differences above 600 Hz are mostly related to noise in the measurements. **Fig. 5** on the other hand tries to quantify the quality of the driving points FRFs: beside any consideration on noise, for a driving point FRF the phase is limited between 0 ^{o} and 180^{o} or, equivalently, the imaginary part should be either always positive or negative. In this case, this assumption generally holds for the majority of the measured driving points FRFs below 1 kHz. It can however be observed that also at lower frequencies some phase values are negative and they will negatively influence the quality of the measured model.

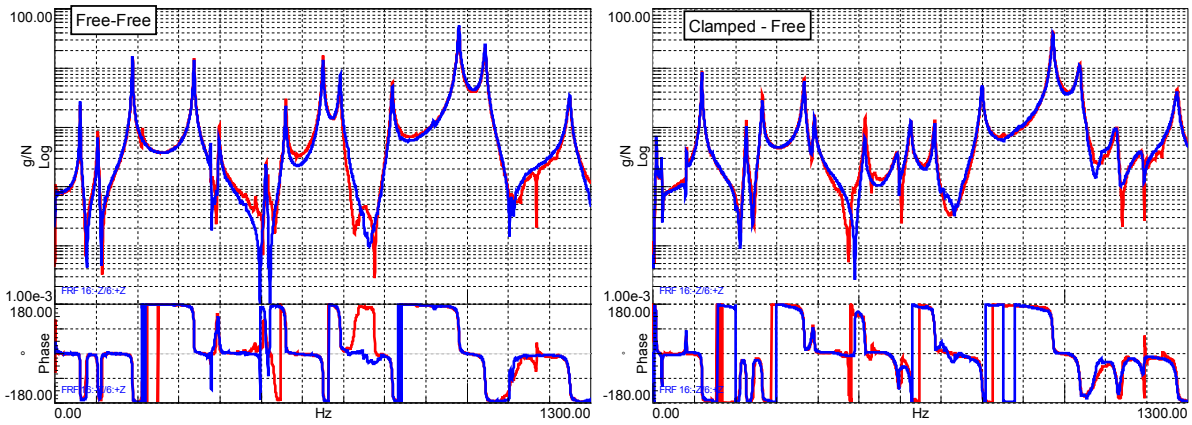

Fig. 4: reciprocity check for both tested boundary conditions.

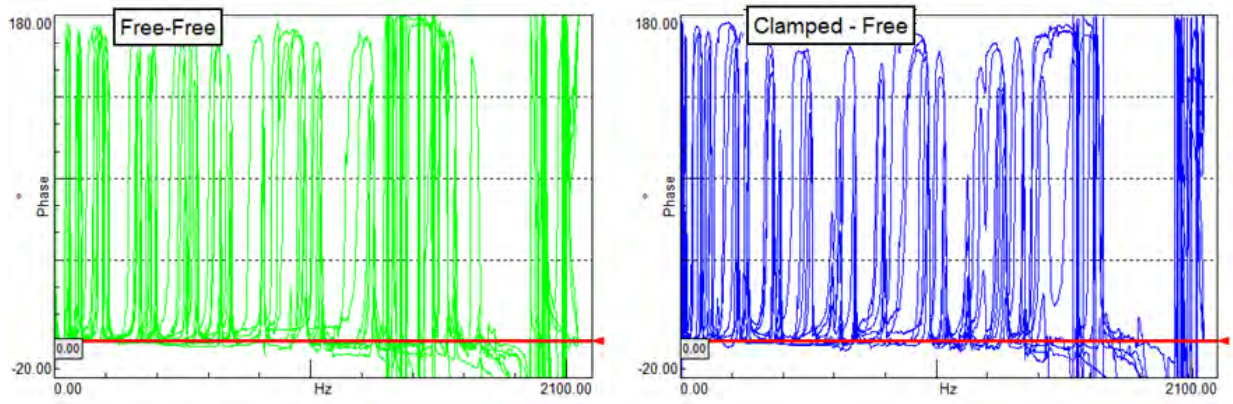

Fig. 5: FRF quality analysis for all driving point FRFs.

3.2 DECOUPLING RESULTS

In general, when performing "standard" FBS according to Eq. 10, all connection DOFs should be measured. There are however many and clear difficulties in measuring these FRFs and, as already discussed in Section 2.2, several decoupling methods have been proposed to compensate for the lack of information. Moreover, only the vertical dynamics of the structure is considered.

As the rotational DOFs at the connection are not measured, all method relying only on connection information (CC, Eq. (10) and AC-C, Eq.(12) will not be discussed here. The analysis will then focus on the results obtained using a combination of connection and internal DOFs for both equilibrium and compatibility (AC-AC Eq. (11)) or only internal (A-A, Eq. (13)). **Fig. 6** shows the results obtained using the measured FRFs, with the assembled and residual substructures in clamped-free as well as free-free boundary condition. In general, it is observed that free-free boundary conditions give better and less noisy results. In both conditions and for both analyzed decoupling techniques, the first peaks are correctly captured. At the third peak around 620 Hz, the FRF becomes noisier and the peak is slightly shifted at higher frequencies. The estimated FRFs start to significantly diverge from the reference one at frequencies above 1000 Hz (corresponding to the dominant peak at the center of the plots). Above, the results have almost no correlation with the behavior of the residual structure. This is also in line with the analysis in Section 3.1 where poor reciprocity and low quality driving point FRFs were discussed at the higher frequencies.

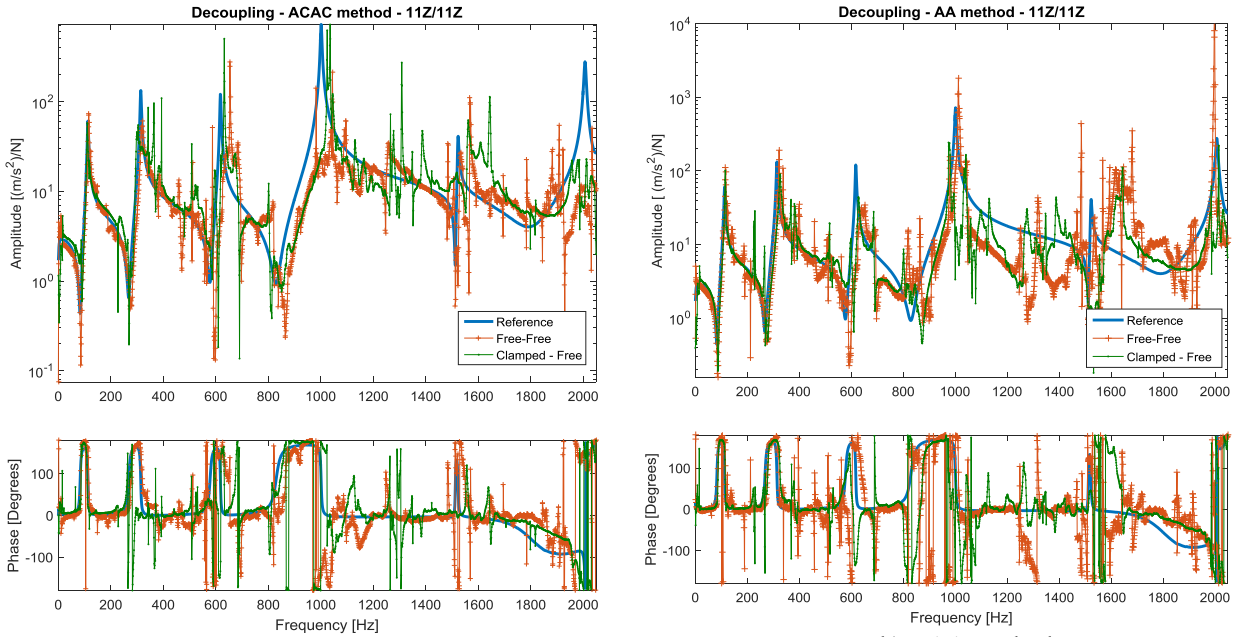

a) ACAC method b) AA method

Fig. 6: Decoupling results at the connection DOF using the measured FRFs directly for both Free-Free and Clamped-Free boundary conditions.

A way to actually assess the results of decoupling is to verify the usability of the calculated FRFs. To do so, a possibility is to use these FRFs for modal identification and then compare the identified modal model with the one obtained by processing the measured FRFs on the beam. To fit a modal model on FRFs, some strict assumptions need to be satisfied which are related to the nature of the model. The noise in the decoupled FRFs is mainly related to the high condition number in the inversion process, which then propagate into the results. As the inversion is performed per frequency line, the objective here is to show that still some consistent and useful information can be derived from decoupling by means of modal analysis. In this process, the PolyMAX identification algorithm will be applied to the whole [4x4] FRF matrix of the residual structure. The identified modal parameters are shown in Table 2. In general, there is a frequency shift in the decoupled FRFs, which can be related to some measurement error or mass loading (e.g. different suspension or cabling in the different setups). However, despite the noise in the estimated FRFs, the dominant modes can still be identified and the damping is comaparable to the original one. The mode at 942.4 Hz which is only identified using the reference FRFs is the beam torsion, that is lowly excited in the implemented setup.

Table 2: Modal Parameter of Substructure B: reference model vs. decoupled FRFs.

Reference		**Free Free ACAC**		**Clamp-Free ACAC**		**Free Free AA**		**Clamp-Free AA**	
Freq.	Damp.	Freq.	Damp.	Freq.	Damp.	Freq.	Damp.	Freq.	Damp.
112.2	0.27	115.8	0.1	110.1	0.11	116.5	0.05	114.7	0.09
313.7	0.06	319.4	0.1	300.3	0.03	321.9	0.02	326.1	0.08
617.2	0.02	648.8	0.02	631.7	0	639.5	0.05	517	0.04
942.4	0.35	/	/	/	/	/	/	/	/
1000.8	0.08	1047	0.04	1042.5	0	1012.2	0	997.6	0.04

Fig. 7 shows the results of applying MAC analysis to the modes obtained from decoupling FRFs using the ACAC method for both considered boundary conditions. In general, the first 3 bending modes are captured correctly. The 5th mode, corresponding to the 4th bending, is also generally identified with a MAC above 70%. The significant off-diagonal high correlation is related to the limited number of sensors used (only 4) to characterize each mode, and could also be observed in the reference data set autoMAC. The MAC analysis on the AA decoupled FRFs slightly less good, identifying the same modes but with less correlation to the original data.

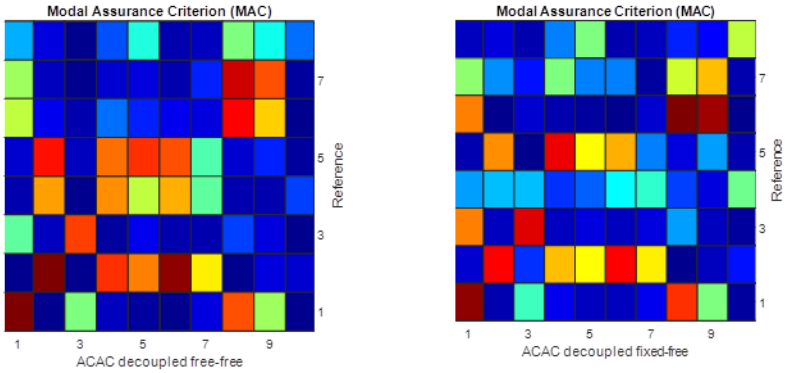

Fig. 7: MAC analysis between reference modes and those obtained by applying experimental modal analysis on decoupled FRFs.

A possible improvement of the proposed method is to use the AC-AC decoupling method and optimize the number and locations of internal points of A used. Assuming this is a planar problem, the connection DOFs that need to be considered is 3, thus, as me measure only the acceleration in the Z direction, a minimum of 2 additional points should be used in the problem. However, in such application over-determination is generally used to improve the accuracy of the matrix inversion. The FRFs from free-free boundary conditions are here analyzed and, as internal dofs on substructure A, the following combinations are analyzed:

- Points 3, 6, 9;
- Points 3,6,10;

- Points 3,9,10;
- Points 6,9,10.

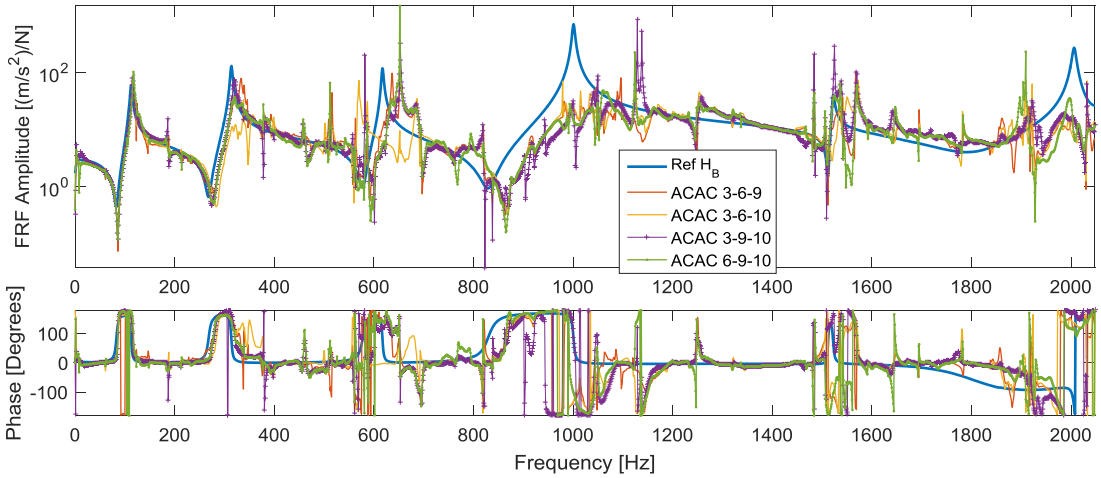

Fig. 8: AC-AC Decoupling results when using only a subset of internal points on substructure A.

As can be observed in **Fig. 8**, the best results for the connection FRF on point B are obtained with the subsets 6-9-10, while for the others the results are comparable if the whole frequency range is taken into account. These results are also confirmed when applying Polymax on the decoupled FRFs. While the case 3-6-10 is not considered as it gives the worst FRFs, the others give generally comparable results Table 3, but the best correlation for the mode shapes is obtained with subset 6-9-10. In general, the 3rd mode is the most difficult to identify. Using the whole set of points or just a limited one doesn't significantly improve the quality of the results, but it shows how the measurement points can be optimally chosen without influencing the quality of the decoupling. On the other hand, by defining adequate pre-test procedures based on numerical models, it is expected that not only the effort can be minimized but also the quality of the results increased.

Table 3: Natural frequencies and damping for different combination of internal points on A for ACAC method.

6-9-10		**3-6-9**		**3-9-10**	
Freq.	Damp.	Freq.	Damp.	Freq.	Damp.
117.4	0.07	116.1	0.13	115.4	0.1
322.5	0.15	327.1	0.07	322.5	0.1
652.0	0	637.0	0.03	649.3	0
/	/	/	/	/	/
1047.1	0	1047.3	0	1017.4	0.09

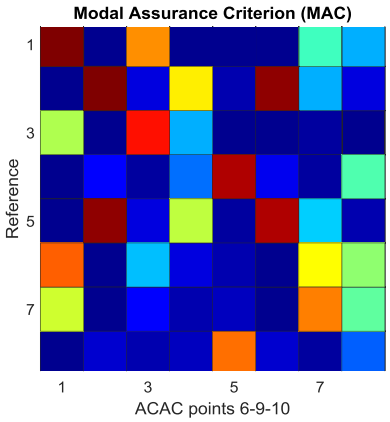

Fig. 9: MAC matrix between references modes and identified modes from ACAC decoupling using internal points of A 6-9-10.

3.3 IMPROVED FRFs FOR DECOUPLING

As two of the main causes that negatively affect the result of decoupling are noise in the measured data and limited reciprocity in the measured FRFs, some methods to improve these FRFs will be here discussed. In particular, three solutions will be here investigated:

- Reduce noise in the FRFs by using a synthesized model obtained from modal fitting with standard Polymax;
- Impose reciprocity by copying the FRFs on the lower diagonal on the upper diagonal and viceversa;

- Use the new modal analysis algorithm proposed in [16] and [17] imposing FRF reciprocity as an additional constraint on the sought modal model.

Decoupling using synthesized input FRFs

The first method to improve the results of decoupling is based on the use of synthesized FRFs to reduce noise and condition number in the inversion. Only the case with free-free boundary conditions is here considered. First, Polymax was applied on the full measured FRF matrices of the assembly and residual structure A. Since the roving hammer approach was used to measure the FRFs, small inconsistencies may appear, resulting is a not very clear stabilization diagram. However, by processing the full FRF matrix, these inconsistencies can be removed imposing the same pole on all curves. The synthesized model will not be the best achievable and mode shapes may also be affected, but on the other hand, for substructuring purpose, noise reduction and consistency may play a much stronger role. The synthesized FRFs were then used for decoupling and the ACAC method was applied.

The results are shown in **Fig. 10**. The decoupled FRFs are now less noisier and with less numerical spikes, but on the other hand they start diverging from the true behavior already at 600 Hz (3rd bending). However, in terms of MAC between the two mode sets, except the torsion mode, relatively good correlation can be found up to the 6th mode (5th bending). On the other hand, the frequency difference is now higher than the results listed in Table 2.

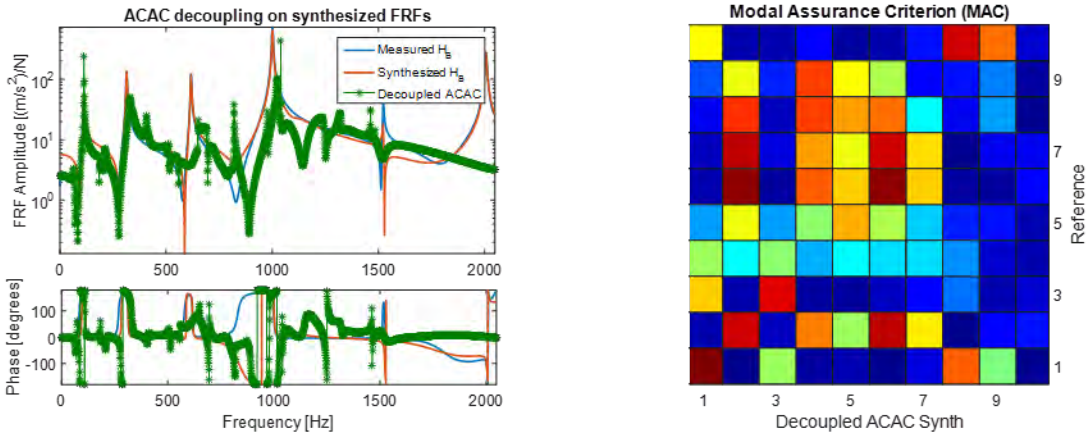

Fig. 10: Decoupling results using synthesized input FRFs. Left: Decoupled FRF. Right: MAC reference and decoupled modal models.

Decoupling imposing reciprocity on input FRFs

Reciprocity of the FRFs matrix is a fundamental assumption in all structural dynamics applications. Although Polymax was applied in the previous paragraph to the complete FRFs matrix, the synthesized model doesn't lead to reciprocal synthesized FRFs. Although there is the possibility to make the synthesized FRFs matrix symmetric after the modal model has been calculated, this process will ignore the lower and upper residuals, that have also a strong effect on decoupling. As a first solution, to impose reciprocity, we will impose the element of the lower diagonal of the measured FRF matrix on the upper diagonal and viceversa. This will not solve all inconsistencies (the elements on the main diagonal are unchanged) but should lead to a more consistent model

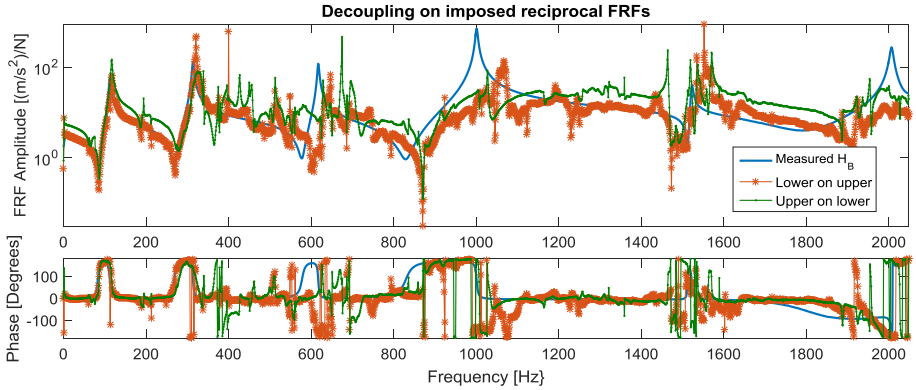

Fig. 11: Decoupling results making the input FRF matrix reciprocal.

The results are shown in Fig. **11**. The quality of the substructured FRFs are similar to those shown in Fig. **6** obtained by processing the raw FRFs. Imposing reciprocity by just changing the elements in the matrix is not improving the results and, morevoer, applying modal analysis on these FRFs only gives good results for the first two modes. Fitting the FRFs with Polymax after imposing reciprocity doesn't help but on the contrary make the results worse.

Decoupling imposing synthesized FRFs with the ML-MM method

The final method investigated in this paper to improve the quality of the decoupled FRFs is to combine the two previous methods (imposing reciprocity and using synthesized FRFs to reduce noise) by using the recently developed multivariable frequency-domain maximum likelihood estimator based on a modal model presented in [16] and further improved and validated in [17]. This method estimates the parameters of a modal model directly instead of identifying a rational fraction polynomial model. Polymax or other standard modal parameter estimation techniques are still used to derive an initial modal model, which the ML-MM method will then optimize to better fit the data. The method is particularly suited for noisy datasets, when the input data are inconsistent, modes are highly damped or the number of input is high. Particularly useful for this application is also the possibility to impose that the resulting modal model is reciprocal as a constraint in the optimization process.

First, the measured FRFs on the assembled structure AB and substructure A are processed using the ML-MM method imposing reciprocity constraints. **Fig. 12** shows the results of the method for one FRF on substructure A, comparing the measured FRF with the initial fit and with the ML-MM fit after the iterations on the modal model are performed. Although with standard Polymax the fit was sometimes better, it should be remembered that here the reciprocity of the modal model was imposed as a constraint and, for inconsistent data, this can results in a lower correlation with the measured data. Also, the analysis focused only on frequencies below 1400 Hz, as it was already observed that above decoupling didn't give satisfactory results.

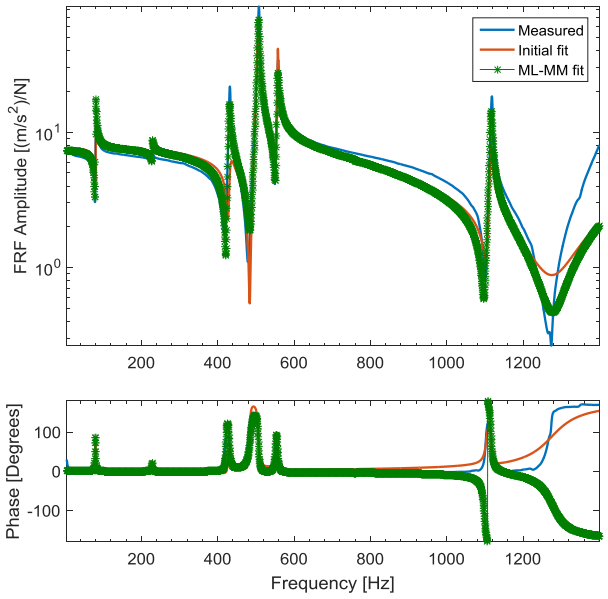

Fig. 12: Example of using ML-MM method with reciprocity constraint on one FRF of substructure A.

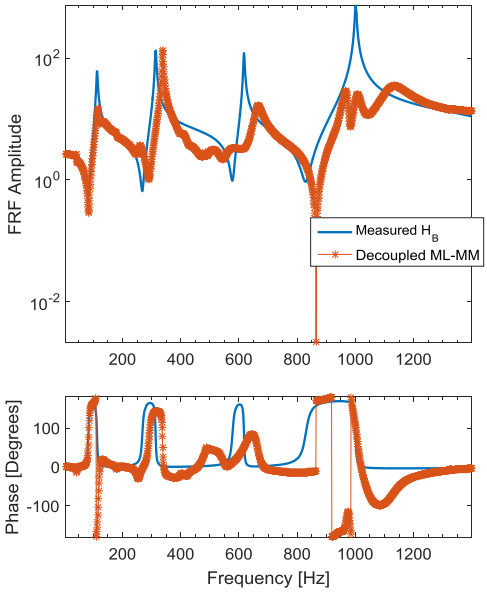

Fig. 13: Decoupling results using ML-MM processed FRFs

The decoupling results are shown in **Fig. 13**. The FRFs are now much smoother in the whole frequency band, but significant deviations can be observed already as of 400 Hz. Polymax is then applied to the decoupled FRFs and the results are again compared with the reference one from the measured FRFs. The obtained results are shown in **Fig. 14** and Table 4. In general, higher differences in the identified modal frequencies are observed, also compared with the results discussed in the previous sections. In terms of modes, except the first one, the other 4 correlate quite well with the original one. In conclusion, although the FRFs are cleaner and reciprocity is enforced in the model, the results are not improving as one might have expected.

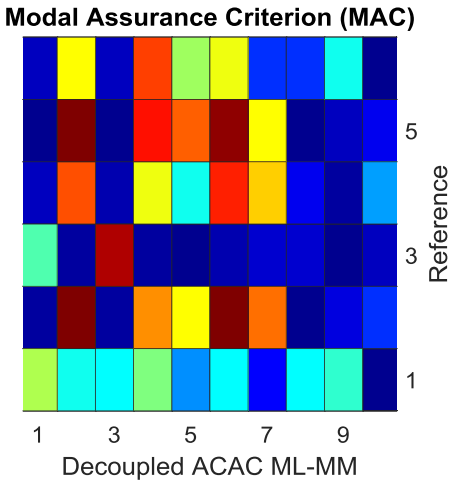

Fig. 14: MAC between reference modes and those from decoupling FRFs process with ML-MM.

Table 4: Comparison between reference modal parameters and those from decoupling FRFs process with ML-MM.

Reference		**ACAC ML-MM**	
Freq.	Damp.	Freq.	Damp.
112.2	0.27	122.8	1.1
313.7	0.06	337.1	0.06
617.2	0.02	663.5	0.19
942.4	0.35	952.9	0.17
1000.8	0.08	1006	0.11

4. CONCLUSIONS

The general rules described in literature to apply frequency based dynamic substructuring to experimental data always stress that the quality of the measured FRFs must be significantly higher than those typically used in the context of experimental modal analysis. In this paper, experimental data have been collected, keeping in mind these rules, on a relatively simple aluminum structure to verify the applicability of Frequency Based Substructuring and to test different techniques to try to improve the quality of the results. The analysis focused also on using different boundary conditions to see their influence on the results. First, the results of using standard extended interface methods were presented. Then, a sensitivity study on the internal DOFs of substructure A used to overdetermine the problem was performed, showing that an optimal point selection can improve the quality of the results by reducing the number redundant information. In this perspective, future activities will further investigate this topic to try to develop rules to optimally choose the measurement point to improve the quality of the results, possibly by making use of validated numerical models in a pre-test approach. In the last section of the paper, different methods were tested to improve the quality of decoupling by enforcing reciprocity on the measured FRFs and reducing noise. In all cases, a slight improvement compared to the original results is observed, but these methods are very sensitive to the processing parameters. Also, it should be stressed that FBS generally relies on the fact that by measuring FRFs all information on the structure are present at all frequencies lines; by applying these techniques, however, some of these information might be lost and the relation between the assembled structure and the substructures partially lost. In general, it can be concluded that for this application the quality of the measured data needs to be extremely higher than in other structural dynamic applications and that a-posteriori method have only limited effects on improving the quality of the results. However, despite the decoupled FRFs are often very noisy, modal analysis can still be applied to obtain a model of the decoupled target structure. Beside the investigation of a procedure for the selection of an optimal set of measurement points, future research will aim at investigating statistical method to exploit the sensitivity of frequency based substructuring to errors in the input data and thus deriving a “more probable” set of decoupled FRFs.

ACNOWLEDGEMENTS

This research was conducted in the frame of the project IWT 130936 ADVENT (Advanced Vibration Environmental Testing). The financial support of the IWT (Flemish Agency for Innovation by Science and Technology) is gratefully acknowledged.

REFERENCES

[1] Rohe, D.P., Allen, M.S., “Investigation of the effectiveness of using an experiment to validate experimental substructure models”, Mechanical Systems and Signal Processing, 43, 2014, pp. 192-216

[2] Allen, M.S., Gindlin, H.M., Mayes, R.L., “Experimental modal substructuring to estimate fixed-base modes from a tests on a flexible fixture”, Journal of Sound and Vibration, 330, 2011, pp. 4413-4428.

[3] Peeters, P., Tamarozzi, T., Vanhollebeke, F., Desmet, W., “A robust approach for substructure decoupling”, Proceedings of the International Seminar on Modal Analysis (ISMA), Leuven, Belgium, 2014.

[4] De Klerk, D., Rixen, D., Voormeeren, S. N., “General framework for dynamic substructuring: history, review and classification of techniques”, AIAA Journal 46(5), 2008, pp. 1169-1181.
[5] Nicgorski, D., Avitabile, P., “Experimental issues related to frequency response function measurements for frequency-based substructuring”, Mechanical Systems and Signal Processing, 24, 2010, pp. 1324-1337.
[6] Rixen, D.J., “How measurement inaccuracies induce spurious peaks in Frequency Based Substructuring”, Proceedings of the International Modal Analysis Conference (IMAC), Jacksonville, USA, 2010.
[7] Jetmundsen B., Biewala R., Flannelly W., “Generalized Frequency Domain Substructure Synthesis”, Journal of American Helicopter Society, 33(1), 1988, pp. 55-65.
[8] Voormeeren, S.N., Rixen, D.J., “A dual approach to substructure decoupling techniques”, Proceedings of the International Modal Analysis Conference (IMAC), Jacksonville, USA, 2010.
[9] D’Ambrogio, W., Fregolent, A., “The role of interface DoFs in decoupling of substructures based on the dual domain decomposition”, Mechanical Systems and Signal Processing, 24(7), 2010, pp. 2035-2048.
[10] De Klerk, D., Rixen, D., Voormeeren, S. N., Pasteuning, F., “Solving the RDoF problem in experimental dynamic substructuring”, Proceedings of the International Modal Analysis Conference (IMAC), Orlando, USA, 2008.
[11] Choi, H.G., Thite, A.N., Thompson D.J., “A threshold for the use of Tikhonov regularization in inverse force determination”, Applied Acoustics, 67, 2006, pp. 700-719.
[12] Nicgorski, D. and Avitabile, P., “Experimental issues related to frequency response measurements for frequency-based substructuring”, Mechanical Systems and Signal Processing, 24, 2010, pp. 1324-1337.
[13] Manzato, S., Risaliti, E., Napoli, C., Tamarozzi, T., Peeters, B., “A review of Frequency-based Substructuring methods and their applicability to Eengineering structures”, Proceedings of the International Conference on Structural Engineering Dynamics (ICEDyn) 2015, Lagos, Portucal, 2015.
[14] Milana,S., Fregolent, A., and Culla, A., “Observation dofs optimization for structural forces identification”, Model Validation and Uncertainty Quantification, Conference Proceedings of the Society for Experimental Mechanics Series, 3, 2015, pp. 27-34.
[15] D'Ambrogio, W., and Fregolent,A., “Ignoring rotational dofs in decoupling structures connected through flexotorsional joints”, Dynamics of Coupled Structures, Conference Proceedings of the Society for Experimental Mechanics Series, 4, 2015, pp. 57-69.
[16] El-Kafafy M., De Troyer T., Peeters B., and Guillaume P., “Fast Maximum-Likelihood Identification of Modal Parameters with Uncertainty Intervals: a Modal Model-Based Formulation”, Mechanical System and Signal Processing, 37, 2013, p. 422-439.
[17] El-Kafafy, M.E., Accardo, G., Peeters, B., Janssens, K., De Troyer, T., Guillaume P., “A Fast Maximum Likelihood-Based Estimation of a Modal Model”, Proceedings of the International Modal Analysis Conference (IMAC), Orlando, USA, 2015.